Inorg. Chem. **2006**, *45*, 5057–5065

Formation, Spectral, Electrochemical, and Photochemical Behavior of Zinc N-Confused Porphyrin Coordinated to Imidazole Functionalized Fullerene Dyads

Francis D'Souza,*,† Phillip M. Smith,† Lisa Rogers,† Melvin E. Zandler,† D.-M. Shafiqul Islam,‡ Yasuyaki Araki,‡ and Osamu Ito*,‡

Department of Chemistry, Wichita State University, 1845 Fairmount, Wichita, Kansas 67260-0051, and Institute of Multidisciplinary Research for Advanced Materials, Tohoku University, Katahira, Sendai, 980-8577, Japan

Received January 30, 2006

Donor–acceptor dyads were constructed using zinc N-confused porphyrin (ZnNCP), a structural isomer of zinc tetraphenylporphyrin, as a donor, and fullerene as an electron acceptor. Two derivatives, pyridine-coordinated zinc N-confused porphyrin (Py:ZnNCP) and the zinc N-confused porphyrin dimer (ZnNCP-dimer) were utilized to form the dyads with an imidazole-appended fulleropyrrolidine (C_{60}Im). These porphyrin isomers formed well-defined 1:1 supramolecular dyads (C_{60}Im:ZnNCP) via axial coordination. The dyads were characterized by optical absorption and emission, ESI-mass, ^{1}H NMR, and electrochemical methods. The binding constant, *K*, was found to be 2.8×10^4 M^{-1} for C_{60}Im:ZnNCP. The geometric and electronic structure of C_{60}Im:ZnNCP were probed by using DFT B3LYP/3-21G(*) methods. The HOMO was found to be on the ZnNCP entity, while the LUMO was primarily on the fullerene entity. The electrochemical properties of C_{60}Im:ZnNCP was probed using cyclic voltammetry in *o*-dichlorobenzene, 0.1 *n*-Bu_4NClO_4. The Py:ZnNCP was found to be easier to oxidize by over 340 mV compared to Py:ZnTPP. Upon dyad formation via axial coordination, the first oxidation revealed an anodic shift of nearly 90 mV. Evidence of photoinduced charge separation from the singlet excited ZnNCP to the appended fullerene was established from time-resolved emission and nanosecond transient absorption studies.

Introduction

Donor−acceptor dyads capable of undergoing photoinduced energy or electron transfer are of current interest for the construction of molecular electronic devices and light energy harvesting systems.[1,2] Fullerenes[3] have been shown to be good candidates for electron acceptors due to their low reduction potentials,[4] three-dimensional structure,[5] and low reorganization energy involved in electron-transfer reactions.[6] Porphyrins[7] have been utilized as electron donors due to their intense absorption in the visible region and due to the fact that they are easily oxidized. Consequently, extensive studies have been performed on covalently linked and self-assembled donor−acceptor dyads composed of porphyrin and fullerene as donor and acceptor entities.[1,2]

Recent advances in the synthesis of different porphyrin isomers, viz. porphycene, corrphycene, hemiporphycene, isoporphycene, and N-confused porphyrins (NCP), differing in the numbers and positions of the pyrrole linkage carbon atoms, have led to these compounds in high yield and purity.[8,9] Studies have revealed some unique properties, different from, and in some cases superior to, those of

* To whom correspondence should be addressed. E-mail: Francis.DSouza@wichita.edu (F.D.); ito@tagen.tohoku.ac.jp (O.I.).
† Wichita State University.
‡ Tohoku University.

(1) (a) Maruyama, K.; Osuka, A. *Pure Appl. Chem*. **1990**, *62*, 1511. (b) Gust, D.; Moore, T. A. *Science* **1989**, *244*, 35. (c) Gust, D.; Moore, T. A.; Moore, A. L. *Acc. Chem. Res*. **1993**, *26*, 198. (d) Wasielewski, M. R. *Chem. Rev*. **1992**, *92*, 435. (e) Paddon-Row: M. N. *Acc. Chem. Res*. **1994**, *27*, 18. (f) Sutin, N. *Acc. Chem. Res*. **1983**, *15*, 275. (g) Meyer, T. J. *Acc. Chem. Res*. **1989**, *22*, 163. (h) Piotrowiak, P. *Chem. Soc. Rev*. **1999**, *28*, 143. (i) El-Khouly, M. E.; Ito, O.; Smith, P. M.; D'Souza, F. *J. Photochem. Photobiol. C: Rev*. **2004**, *5*, 79−104. (j) Guldi, D. M. *Chem. Commun*. **2000**, 321. (k) Gust D.; Moore, T. A. In *The Porphyrin Handbook*; Kadish, K. M., Smith, K. M., Guilard, R., Eds.; Academic Press: Burlington, MA, 2000; Vol. 8, pp 153−190. (l) Imahori, H.; Sakata, Y. *Adv. Mater*. **1997**, *9*, 537. (m) Connolly, J. S.; Bolton, J. R. In *Photoinduced Electron Transfer*; Fox, M. A., Chanon, M., Eds.; Elsevier: Amsterdam, 1988; Part D, pp 303−393.

10.1021/ic0601687 CCC: $33.50
Published on Web 05/12/2006

porphyrins for applications of these molecules.[10,11] However, these types of compounds have not been utilized as electron- or energy-donor moieties in donor−acceptor systems, although porphyrinic macrocycles are found in natural light energy harvesting complexes and photosynthetic reaction centers.[12] In continuation of our efforts to build novel molecular and supramolecular donor−acceptor systems, in the present study, we have explored using one of the structural isomers of *meso*-tetraphenylporphyrin, N-confused tetraphenylporphyrin (also called 2-aza-21-carba-5,10,15,20-tetraarylporphyrin and inverted tetraphenylporphyrin)[9] as a donor entity, and have developed donor−acceptor dyads using a functionalized fullerene. The utilized N-confused tetraphenylporphyrin differs structurally from the familiar tetraphenylporphyrin by inversion of one of the pyrrole rings, resulting in three N atoms and one C atom at the macrocycle core, and the inverted nitrogen at a β-position of the periphery of the macrocycle. Because of the similarity of the inner framework to porphyrins, the coordination chemistry of these isomers is expected to be closely related; however, owing to the presence of the outward-facing nitrogen, different extended coordination geometries can also be expected. For example, the target molecule in the present study, zinc N-confused tetraphenylporphyrin, can bind two metal ions both inside and outside of the porphyrin core due to the available inner and outer nitrogens. Thus, they serve as new scaffolds for building supramolecular architectures. Recently, Furuta et al.[13] explored such coordination chemistry and reported the syntheses and characterization of tetranuclear and dinuclear zinc(II) N-confused dimers (ZnNCP-dimer) and a pyridine-coordinated zinc(II) monomer complex (Py:ZnNCP). Here, we have utilized the ZnNCP-dimer and Py:ZnNCP to build the donor−acceptor dyads.

Scheme 1

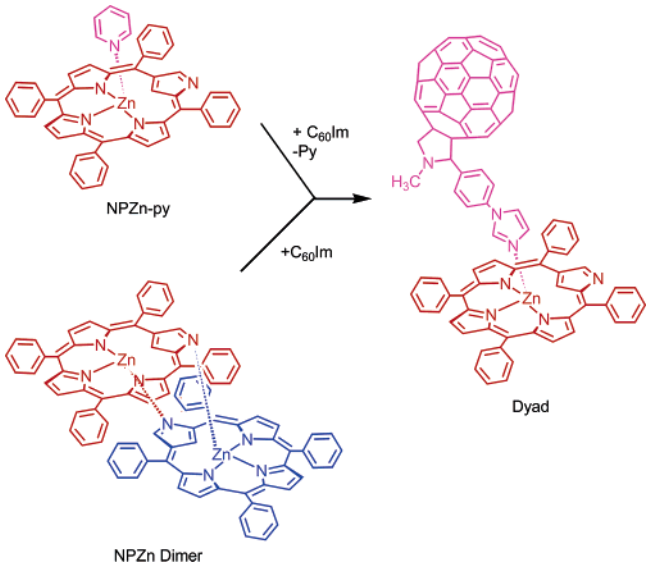

The methodology adopted for the formation of the donor−acceptor dyads is shown in Scheme 1. The first method involves Py:ZnNCP with an imidazole-appended fulleropyrrolidine (C_{60}Im). Because of the better coordinating ability, the imidazole replaces the bound pyridine, thus forming the dyad via axial coordination (C_{60}Im:ZnNCP).[14] In the second method, C_{60}Im breaks the external coordinated Zn−N bonds of the ZnNCP-dimer and forms the dyad via axial ligation of C_{60}Im. Systematic studies have been performed to characterize these dyads and their ability to undergo light-induced electron-transfer reactions.

(2) (a) Ward, M. W. *Chem. Soc. Rev.* **1997**, *26*, 365. (b) Hayashi, T.; Ogoshi, H. *Chem. Soc. Rev.* **1997**, *26*, 355. (c) Sessler, J. S.; Wang, B.; Springs, S. L.; Brown, C. T. In *Comprehensive Supramolecular Chemistry*; Atwood, J. L., Davies, J. E. D., MacNicol, D. D., Vögtle, F., Eds.; Pergamon: Elmsford, NY, 1996; Chapter 9. (d) D'Souza, F.; Ito, O. *Coord. Chem. Rev.* **2005**, *249*, 1410. (e) Sanchez, L.; Martin, N.; Guldi, D. M. *Angew. Chem., Int. Ed.* **2005**, *44*, 5374. (f) *Introduction of Molecular Electronics*; Petty, M. C., Bryce, M. R., Bloor, D., Eds.; Oxford University Press: New York, 1995.

(3) (a) Kroto, H. W.; Heath, J. R.; O'Brien, S. C.; Curl R. F.; Smalley, R. E. *Nature* **1985**, *318*, 162. (b) Kratschmer, W.; Lamb, L. D.; Fostiropoulos F.; Huffman, D. R. *Nature* **1990**, *347*, 345.

(4) Xie, Q.; Perez-Cordero, E.; Echegoyen, L. *J. Am. Chem. Soc.* **1992**, *114*, 3978.

(5) *Fullerene and Related Structures*; Hirsch, A., Ed.; Springer: Berlin, 1999; Vol. 199.

(6) Imahori, H.; Hagiwara, K.; Akiyama, T.; Akoi, M.; Taniguchi, S.; Okada, S.; Shirakawa, M.; Sakata, Y. *Chem. Phys. Lett.* **1996**, *263*, 545.

(7) (a) *The Porphyrin Handbook*; Kadish, K. M., Smith, K. M., Guilard, R., Eds.; Academic Press: Burlington, MA, 2000; Vol. 1−10. (b) Smith, K. M. *Porphyrins and Metalloporphyrins*; Elsevier: New York, 1977.

(8) (a) Vogel, E.; Kocher, M.; Schmickler, H.; Lex, J. *Angew. Chem., Int. Ed. Engl.* **1986**, *25*, 257. (b) Sessler, J. L.; Bruker, E. A.; Weghorn, S. J.; Kisters, M.; Schafer, M.; Lex, J.; Vogel, E. *Angew. Chem., Int. Ed. Engl.* **1994**, *33*, 2308. (c) Aukauloo, M. A.; Guilard, R. *New J. Chem.* **1994**, *18*, 1205. (d) Callot, H. J.; Rohrer, A.; Tschamber, T. *New J. Chem.* **1995**, *19*, 155. (e) Vogel, E.; Scholz, P.; Demuth, R.; Erben, E.; Broring, M.; Schmickler, H.; Lex, J.; Hohlneicher, G.; Bremm, D.; Wu, Y.-D. *Angew. Chem., Int. Ed.* **1999**, *38*, 2919.

(9) (a) Furuta, H.; Asano, T.; Ogawa, T. *J. Am. Chem. Soc.* **1994**, *116*, 767. (b) Chmielewski, P. J.; Latos-Grazù yn'ski, L.; Rachlewicz, K.; G×b8owiak, T. *Angew. Chem., Int. Ed. Engl.* **1994**, *33*, 779. (c) Srinivasan, A.; Furuta, H.; Osuka, A. *Chem. Commun.* **2001**, 1666. (d) Furuta, H.; Kubo, N.; Maeda, H.; Ishizuka, T.; Osuka, A.; Nanami, H.; Ogawa, T. *Inorg. Chem.* **2000**, *39*, 5424.

(10) (a) D'Souza, F.; Boulas, P.; Aukauloo, A. M.; Guilard, R.; Kisters, M.; Vogel, E.; Kadish, K. M. *J. Phys. Chem.* **1994**, *98*, 11885. (b) Kadish, K. M.; Caemelbecke, E. V.; Boulas, P.; D'Souza, F.; Vogel, E.; Kisters, V.; Medforth., C.; Smith, K. M. *Inorg. Chem.* **1993**, *32*, 4177. (c) Kadish, K. M.; D'Souza, F.; Van Caemelbecke, E.; Boulas, P.; Vogel, E.; Aukauloo, A. M.; Guilard, R. *Inorg. Chem.* **1994**, *33*, 4474.

(11) (a) Parusel, A. B. J.; Ghosh, A. *J. Phys. Chem. A* **2000**, *104*, 2504. (b) Ghosh, A.; Wondimagegn, T.; Nilsen, H. *J. Phys. Chem. B* **1998**, *102*, 10459. (c) Zandler, M. E.; D'Souza, F. *J. Mol. Struct. (THEOCHEM)* **1997**, *401*, 301. (d) Szterenberg, L.; Latos-Grazynski, L. *Inorg. Chem.* **1997**, *36*, 6287. (14) (e) Furuta, H.; Ishizuka, T.; Osuka, A.; Dejima, H.; Nakagawa, H.; Ishikawa, Y. *J. Am. Chem. Soc.* **2001**, *123*, 6207. (f) Belair, J. P.; Ziegler, C. S.; Rajesh, C. S.; Modarelli, D. A. *J. Phys. Chem. A* **2002**, *106*, 6445. (g) Wolff, S. A.; Aleman, E. A.; Banerjee, D.; Rinaldi, P. L.; Modarelli, D. A. *J. Org. Chem.* **2004**, *69*, 4571. (h) Strachan, J.-P.; O'Shea, D. F.; Balasubramanian, T.; Lindsey, J. S. *J. Org. Chem.* **2000**, *65*, 3160. (i) Harvey, J. D.; Ziegler, C. J. *Coord. Chem. Rev.* **2003**, *247*, 1. (k) Shaw, J. L.; Garrison, S. A.; Aleman, E. A.; Ziegler, C. J.; Modarelli, D. A. *J. Org. Chem.* **2004**, *69*, 7423. (j) Morimoto, T.; Taniguchi, S.; Osuka, A.; Furuta, *Eur. J. Org. Chem.* **2005**, 3887. (k) Geier, G. R., III.; Lindsey, J. S. *J. Org. Chem.* **1999**, *64*, 1596−1603.

(12) (a) Deisenhofer, J.; Epp, O.; Miki, K.; Huber, R.; Michel, H. *Nature* **1985**, *318*, 618. (b) Deisenhofer, J.; Michel, H. *Science* **1989**, *245*, 1463. (c) Allen, P.; Feher, G.; Yeates, T. O.; Rees, D. C.; Deisenhofer, J.; Michel, H.; *Proc. Natl. Acad. Sci. U.S.A.* **1986**, *83*, 8589.

(13) Furuta, H.; Ishizuka, T.; Osuka, A. *J. Am. Chem. Soc.* **2002**, *124*, 5622.

(14) (a) D'Souza, F.; Deviprasad, G. R.; Zandler, M. E.; Hoang, V. T.; Arkady, K.; Van Stipdonk, M.; Perera, A.; El-Khouly, M. E.; Fujitsuka, M.; Ito, O. *J. Phys. Chem. A.* **2002**, *106*, 3243. (b) D'Souza, F.; Deviprasad, G. R.; Rahman, M. S.; Choi, J. P. *Inorg. Chem.* **1999**, *38*, 2157. (c) D'Souza, F.; Smith, P. M.; Zandler, M. E.; McCarty, A. L.; Itou, M.; Araki, Y.; Ito, O. *J. Am. Chem. Soc.* **2004**, *126*, 7898.

Experimental Section

Chemicals. Buckminsterfullerene, C_{60} (+99.95%) was from BuckyUSA (Bellaire, TX). *o*-Dichlorobenzene (*o*-DCB), sarcosine, 4-imidozolyl benzaldehyde, pyrrole, benzaldehyde, and methanesulfonic acid were from Aldrich Chemicals (Milwaukee, WI). Tetrabutylammonium perchloride, *n*-Bu_4NClO_4 was from Fluka Chemicals. All chemicals were used as received. Synthesis of C_{60}Im was reported in the literature.[14a] The syntheses of N-confused porphyrin derivatives was accomplished according to a literature procedure with some modifications.[15] The details are given in the Supporting Information.

Instrumentation. The computational calculations were performed by the DFT B3LYP/3-21G(*) method with the GAUSSIAN03 software package[16] on various PCs. The graphics of HOMO and LUMO were generated with the help of GaussView software. The steady-state UV−vis and fluorescence spectra were measured with a Shimadzu Model 1600 UV-vis and a Spex Fluorolog-tau spectrometers, respectively. The ^{1}H NMR studies were carried out either on Varian 400 MHz or 300 MHz spectrometers. Tetramethylsilane (TMS) was used as an internal standard. Cyclic voltammograms were recorded on a EG&G Model 263A potentiostat using a three-electrode system in *o*-DCB containing 0.1 M *n*-Bu_4NClO_4 as the supporting electrolyte. A platinum button or glassy carbon electrode was used as the working electrode. A platinum wire served as the counter electrode, and a Ag/AgCl was used as the reference electrode. The ferrocene/ferrocenium (Fc/Fc^+; 0.59 V vs Ag/AgCl) redox couple was used as an internal standard. All the solutions were purged prior to spectral measurements using argon gas. The ESI-mass spectral analyses of the self-assembled complexes were performed by using a Fennigan LCQ-Deca mass spectrometer. The starting compounds and the dyads (about 0.1 mM concentration) were prepared in CH_2Cl_2, freshly distilled over calcium hydride.

The picosecond time-resolved fluorescence spectra were measured using an argon-ion pumped Ti:sapphire laser (Tsunami; pulse width = 2 ps) and a streak scope (Hamamatsu Photonics; response time = 10 ps). The details of the experimental setup are described elsewhere.[17] Nanosecond transient absorption measurements were carried out using the SHG (532 nm) of an Nd:YAG laser (Spectra Physics, Quanta-Ray GCR-130, fwhm = 6 ns) as the excitation source. For the transient absorption spectra in the near-IR region (600−1600 nm), the monitoring light from a pulsed Xe lamp was detected with a Ge-avalanche photodiode (Hamamatsu Photonics, B2834).

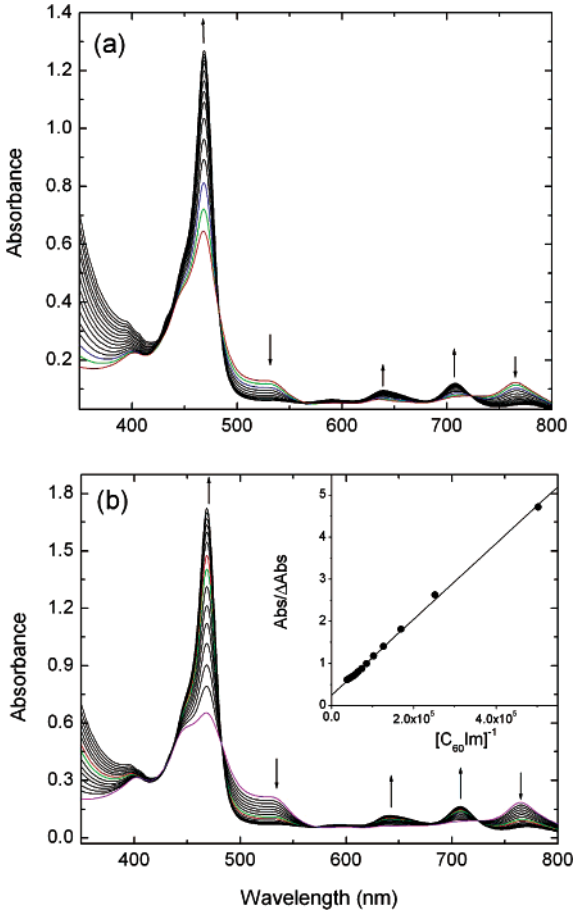

Figure 1. Spectral changes observed during the titration of imidazole-appended fullerene (2.0 μL each addition), C_{60}Im to the solution containing (a) Py:ZnNCP (3.3 μM) and (b) ZnNCP-dimer (3.4 μM) in *o*-dichlorobenzene. The figure b inset shows a Benesi−Hildebrand plot constructed for evaluating the binding constant.

Results

Optical Absorption Studies. The dyad was formed using two different zinc N-confused porphyrin complexes as starting materials (Scheme 1). One of the starting compounds was Py:ZnNCP, and the other was the ZnNCP-dimer. The dyad formation was monitored by UV−visible absorption spectroscopy by adding C_{60}Im to each of the respective starting porphyrins in *o*-DCB (Figure 1). Isosbestic points were observed in the spectrum at 725, 572, and 482 nm. The Soret band located at 467 nm increased in intensity, as well as smaller bands at 641 and 707 nm. Also, bands diminished in intensity at 524 and 764 nm. It is important to note that the final spectrum in Figure 1a and b are identical, indicating the formation of C_{60}Im:ZnNCP as the final species starting from either of the routes shown in Scheme 1.

The spectral intensity changes of the Soret band were used to construct a Benesi−Hildebrand plot,[18] as shown in Figure 1b, inset. The formation constant (*K*) for dyad formation was found to be 2.8×10^4 M^{-1}. This value was approximately

(15) Geier, G. R., III; Haynes, D. M.; Lindsey, J. S. *Org. Lett.* **1999**, *9*, 1455−1458.

(16) Frisch, M. J.; Trucks, G. W.; Schlegel, H. B.; Scuseria, G. E.; Robb, M. A.; Cheeseman, J. R.; Montgomery, J. A., Jr.; Vreven, T.; Kudin, K. N.; Burant, J. C.; Millam, J. M.; Iyengar, S. S.; Tomasi, J.; Barone, V.; Mennucci, B.; Cossi, M.; Scalmani, G.; Rega, N.; Petersson, G. A.; Nakatsuji, H.; Hada, M.; Ehara, M.; Toyota, K.; Fukuda, R.; Hasegawa, J.; Ishida, M.; Nakajima, T.; Honda, Y.; Kitao, O.; Nakai, H.; Klene, M.; Li, X.; Knox, J. E.; Hratchian, H. P.; Cross, J. B.; Bakken, V.; Adamo, C.; Jaramillo, J.; Gomperts, R.; Stratmann, R. E.; Yazyev, O.; Austin, A. J.; Cammi, R.; Pomelli, C.; Ochterski, J. W.; Ayala, P. Y.; Morokuma, K.; Voth, G. A.; Salvador, P.; Dannenberg, J. J.; Zakrzewski, V. G.; Dapprich, S.; Daniels, A. D.; Strain, M. C.; Farkas, O.; Malick, D. K.; Rabuck, A. D.; Raghavachari, K.; Foresman, J. B.; Ortiz, J. V.; Cui, Q.; Baboul, A. G.; Clifford, S.; Cioslowski, J.; Stefanov, B. B.; Liu, G.; Liashenko, A.; Piskorz, P.; Komaromi, I.; Martin, R. L.; Fox, D. J.; Keith, T.; Al-Laham, M. A.; Peng, C. Y.; Nanayakkara, A.; Challacombe, M.; Gill, P. M. W.; Johnson, B.; Chen, W.; Wong, M. W.; Gonzalez, C.; Pople, J. A. *Gaussian 03*, revision B.04; Gaussian, Inc.: Wallingford, CT, 2004.

(17) (a) Matsumoto, K.; Fujitsuka, M.; Sato, T.; Onodera, S.; Ito, O. *J. Phys. Chem. B* **2000**, *104*, 11632. (b) Komamine, S.; Fujitsuka, M.; Ito, O.; Morikawa, K.; Miyata, T.; Ohno, T. *J. Phys. Chem. A* **2000**, *104*, 11497.

(18) Benesi, H. A.; Hildebrand, J. H. *J. Am. Chem. Soc*. **1949**, *71*, 2703.

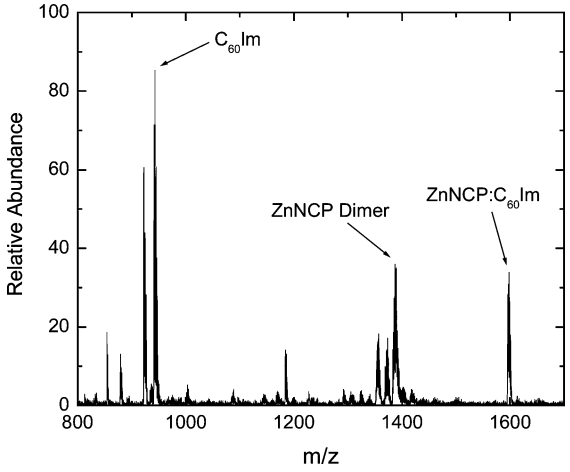

Figure 2. ESI-mass of the C_{60}Im:ZnNCP dyad (0.05 mM) in CH_2Cl_2.

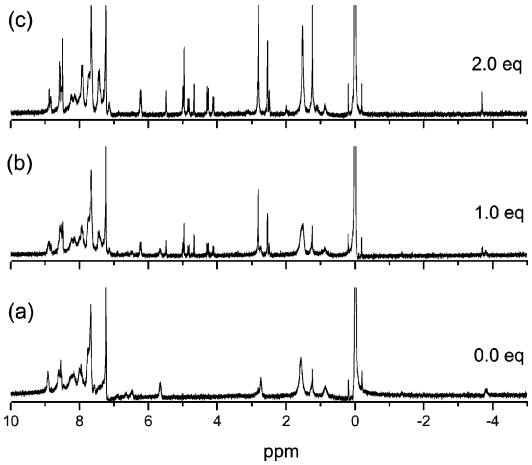

Figure 3. ^{1}H NMR spectrum of (a) ZnNCP (0.05 mM), (b) ZnNCP + C_{60}Im (0.05 mM each), and (c) ZnNCP (0.05 mM) + C_{60}Im (0.1 mM) in $CDCl_3$.

twice that reported earlier for the zinc porphyrin counterpart donor−acceptor dyad ($K = 1.2 \times 10^4$ M^{-1}).[14a] This is expected because the axial bond in C_{60}Im:ZnNCP makes zinc tetracoordinated (ignoring the macrocycle Zn−C bond), while in the previously studied system, the axial bond is the fifth bond to the zinc porphyrin core. Also, a Jobs plot of the UV−visible absorption data confirmed 1:1 complex formation.

Formation of the 1:1 dyad was also confirmed by ESI-mass spectrometry. The respective porphyrin starting complexes were mixed with stoichiometric amounts of C_{60}Im in CH_2Cl_2. The spectra for each experiment revealed the predicted peak corresponding to the dyad at $m/z = 1597.9$ as shown in Figure 2 for the respective ZnNCP-dimer interacting with C_{60}Im. Also, the cluster of peaks revealed the predicted isotopic abundance expected for the dyad.

^{1}H NMR Studies. Figure 3a shows the ^{1}H NMR spectrum of the Py:ZnNCP complex. The C−H proton in the interior of the ring showed up as a broad singlet at −3.79 ppm. The two *o*-pyridine protons, *m*-pyridine protons, and *p*-pyridine proton showed up as broad singlets at 2.72, 5.66, and 6.49 ppm, respectively. The protons were shifted upfield as compared to that of unbound pyridine as a result of the ring current effects of the porphyrin. Upon addition of 1 equiv of C_{60}Im (Figure 3b), the interior C−H proton became split, giving rise to a new singlet at −3.71 ppm which corresponds to that of the C_{60}Im-bound species. Also, two sets of fulleropyrrolidine peaks appeared in the spectrum which corresponds to the "bound" and "free" C_{60}Im. The "free" C_{60}Im fulleropyrrolidine peaks showed up at (N−CH_3) 2.82, a doublet at 4.29, and a singlet and doublet buried together at 4.95 ppm. The "bound" C_{60}Im fulleropyrrolidine peaks showed up at (N−CH_3) 2.55, doublet at 4.09, singlet at 4.64, and a doublet at 4.84 ppm. Two new peaks appear at 5.47 (singlet) and 6.24 (doublet) ppm, which correspond to an imidazole and two phenyl peaks in the "bound" C_{60}Im species, respectively. These peaks are shifted from 7.11 and 7.46 ppm, respectively, as compared to "free" C_{60}Im. The other imadazole and phenyl entity peaks are presumably buried in the aromatic region of the spectrum. Also, the pyridine peaks have decreased in intensity. After 2 equiv of C_{60}Im was added (Figure 3c), the pyridine peaks had completely disappeared from the spectrum and it is assumed that the peaks of the displaced pyridine were buried somewhere in the aromatic peaks of the porphyrin. Also, the peak at −3.79 ppm which corresponds to the pyridine-bound complex completely disappeared and only the new singlet at −3.71 ppm which corresponds to the C_{60}Im-bound complex appeared in the spectrum. These data indicate that the pyridine was displaced from the complex and that the final product was C_{60}Im:ZnNCP.

Computational Studies. The geometry and electronic structure of the dyad was probed by DFT calculations using the B3LYP/3-21G(*) method. The advantages of B3LYP/3-21G(*) in predicting the structures of molecular/supramolecular complexes of the size discussed here have been recently summarized.[21] In our calculations, the starting compounds were fully optimized on a Born−Oppenheimer potential energy surface and allowed to interact. The geometric parameters of the conjugates were obtained after complete energy optimization. Figure 4a shows the structure of Py:ZnNCP. The computed structure agreed well with the X-ray structure reported earlier by Furuta et al.[13] In the computed structure, the zinc atom was pentacoordinated with three pyrrolic nitrogens, one carbon of the N-confused pyrrole, and the nitrogen of the coordinated pyridine. The zinc was 0.4 Å above the plane, and the C−Zn distance and the tilting angle of the confused pyrrole ring were 2.23 Å and 29°, respectively. The zinc was coordinated to the inner CH carbon in a side-on η^1-coordination fashion. Earlier, the tilting of the confused pyrrole ring was attributed to the unfavorable interaction between the fully occupied $d_{x^2-y^2}$ orbital of d^{10} zinc and the sp^2 orbital of the inner carbon.[13] This ultimately resulted into a side-on η^1-type coordination between the carbon and the zinc. The frontier HOMO and LUMO of the investigated complex are also shown in Figure 4a. The first two HOMOs and the first two LUMOs were both π-type orbitals spread all over the macrocycle ring atoms. That is, no localized orbitals on the N-confused

(19) Miller, J. R.; Drough, G. D. *J. Am. Chem. Soc*. **1952**, *74*, 3977.
(20) Nappa, M.; Valentine, J. S. *J. Am. Chem. Soc*. **1978**, *100*, 5075.
(21) Zandler, M. E.; D'Souza, F. *C. R. Chemie* **2006**, in press.

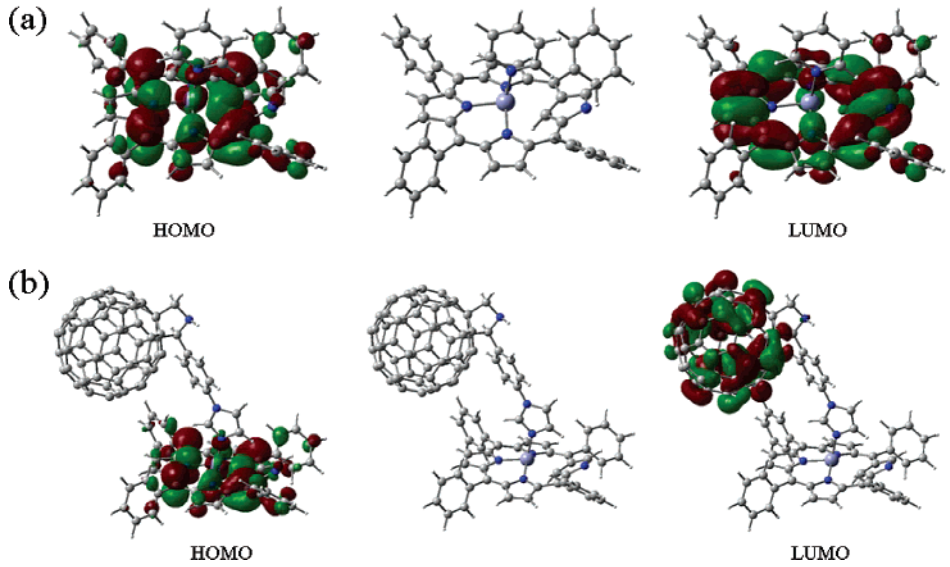

Figure 4. B3LYP/3-21G(*) optimized (a) ZnNCP and (b) dyad formed by axial coordination of imidazole appended fullerene to N-confused tetraphenylporphyrin (C_{60}Im:ZnNCP). The frontier HOMO and LUMO are shown on the left and right sides of each optimized structure, respectively.

pyrrole segment or on the rest of the macrocycle were observed. The computed HOMO−LUMO gap was found to be 2.39 eV, which compared with a HOMO−LUMO gap of 2.78 eV for pyridine coordinated zinc tetraphenylporphyrin.[14a] This HOMO−LUMO gap was also found to be comparable to the HOMO−LUMO gap (2.12 eV) for the free-base N-confused teraphenylporphyrins.[20]

The structure of the B3LYP/3-21G(*) computed supramolecular dyad is shown in Figure 4b. In the computed structure, the newly formed Zn−N distance was found to be 2.01 Å, which was slightly smaller than the Zn−N distances of the macrocycle, which averages of 2.05 Å. Replacing the axial pyridine (Figure 4a) by imidazole ligand in the dyad had little or no effect on the overall geometry of the N-confused porphyrin macrocycle. The edge-to-edge distance and center-to-center distance between the zinc to the fullerene spheroid were found to be 7.60 and 12.43 Å, respectively. These values were comparable to the earlier computed and calculated from X-ray structural studies of ZnTPP−C_{60}Im dyad.[23] That is, the overall geometry of the present dyad is similar to the earlier reported C_{60}Im:ZnNCP dyad. The B3LYP/3-21G(*) calculated HOMO and LUMO for the investigated dyad are shown in Figure 4b. The majority of the HOMO was found to be located on the N-confused porphyrin entity with a small orbital coefficient on the axial imidazole ligand. On the other hand, the majority of the LUMO was located on the C_{60} spheroid. The absence of HOMOs on C_{60} and LUMOs on the porphyrin macrocycle suggests weak charge-transfer-type interactions between the donor and acceptor entities of the dyad in the ground state. The present results also suggest that the charge-separated state is $C_{60}Im^{\bullet-}$:NCPZn$^{\bullet+}$. The orbital energies of the HOMO and the LUMO were found to be −4.38 and −3.56 eV, which resulted in a 'HOMO−LUMO gap' of 0.82 eV. This value was smaller by 0.14 eV when compared to the value calculated for the analogue dyad formed by using zinc tetraphenylporphyrin.[14a]

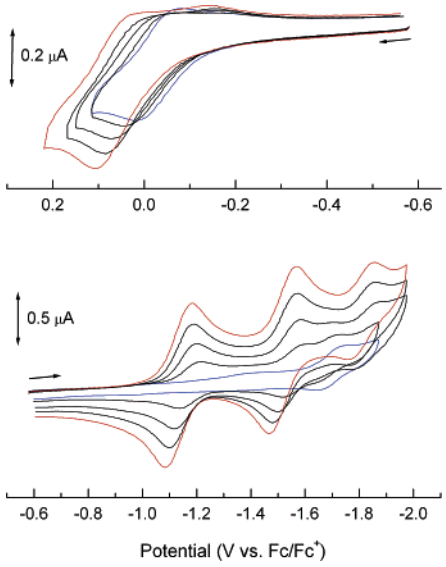

Figure 5. Cyclic voltammograms of Py:ZnNCP on increasing addition of C_{60}Im (0.5 equiv each addition) in *o*-dichlorobenzene, 0.1 (TBA)ClO_4. Scan rate = 100 mV s^{-1}.

Cyclic Voltammetric Studies. To probe the redox properties of the newly formed donor−acceptor dyad and also to verify the theoretical predictions of a smaller HOMO−LUMO gap of the N-confused porphyrin and the resulting dyad, cyclic voltammetric studies were performed in *o*-DCB containing 0.1 M *n*-Bu_4NClO_4. Owing to a similar coordination environment, the electrochemical redox behavior of both the monomer and the dimer was found to be quite similar. Both compounds revealed two one-electron oxidations and two one-electron reductions (see the blue traces in Figure 5). For Py:ZnNCP, the oxidations were located at $E_{1/2}$ = −0.04 and 0.10 V vs Fc/Fc$^+$ and the reductions were located at $E_{1/2}$ = −1.71 and −2.00 V vs Fc/Fc$^+$. It is important to note that the first oxidation potential is close to that of the Fc/Fc$^+$ redox couple and easier to oxidize by 350 mV

(22) Belair, J. P.; Ziegler, C. J.; Rajesh, C. S.; Modarelli, D. A. *J. Phys. Chem. A* **2002**, *106*, 6445.
(23) D'Souza, F.; Rath, N. P.; Deviprasad, G. R.; Zandler, M. E. *Chem. Commun.* **2001**, 267.

compared to the first oxidation potential of the pyridine coordinated zinc tetraphenylporphyrin, Py:ZnTPP.[14a] The easier oxidation of ZnNCP suggests better electron-donating ability of the complex. The electrochemical "HOMO−LUMO gap", that is, the potential difference between the first oxidation and first reduction, was found to be 1.67 eV for Py:ZnNCP which is smaller than the 2.21 eV found for Py:ZnTPP.

The first reversible oxidation and reversible reduction of the dimer were located at $E_{1/2} = -0.07$ and -1.80 V vs Fc/Fc^+, respectively. The electrochemical HOMO−LUMO gap for the ZnNCP-dimer was found to be 1.73 V, smaller than that of Py:ZnTPP. It may be mentioned here that the redox peaks of the dimer did not reveal any splitting, often observed for strongly $\pi-\pi$ interacting porphyrin dimers.[24] These results suggest weak $\pi-\pi$-type interactions between the two macrocycles of the investigated dimer.[13]

The cyclic voltammograms of the dyad formed by titrating Py:ZnNCP with C_{60}Im are shown in Figure 5. Upon addition of C_{60}Im, the first oxidation of ZnNCP shifted to more positive potentials by about 70 mV. The C_{60}Im bound in C_{60}Im:ZnNCP exhibited three reversible reductions within the potential window, the first two of which were located at $E_{1/2} = -1.18$ and -1.57 vs Fc/Fc^+, respectively. The third reduction process had contributions from the third reduction of fullerene and the first reduction of ZnNCP. The first reduction potential corresponding to C_{60}Im in the dyad was not significantly different from the reduction potential of C_{60}-Im obtained in the absence of any donor. The experimentally determined "HOMO−LUMO gap", that is, the difference between the first oxidation potential of the donor, ZnNCP, and the first reduction potential of the acceptor, C_{60}Im, was found to be 1.18 V and was independent of the route followed to form the dyad in Scheme 1. This energy gap compared with an electrochemical energy gap of 1.39 V reported earlier for the C_{60}Im:ZnTPP dyad.[14a] The trends in these results tracked that of the computational results discussed in the previous section. However, the agreement would not be expected to be exact since much of the absolute difference between the experimental and computed results are attributed to their different environments, that is, for the noninteracting or 'gas-phase' environment computation and the solvent *o*-DCB containing *n*-Bu_4NClO_4 for electrochemical measurements.

Fluorescence Emission Studies. Steady-state fluorescence quenching experiments were performed in order to determine the efficiency of quenching of ZnNCP by fullerene. The Py:ZnNCP complex, in *o*-DCB, was excited at 467 nm and the emission spectra were monitored upon addition of fullerene. The emission spectrum of the Py:ZnNCP displayed two intense peaks at 734 and 794 nm, respectively, and a much less intense band around 650 nm (Figure 6a), which were significantly red-shifted from normal zinc porphyrin. The intensity of the emission bands of ZnNCP was found to be smaller than that of an equimolar concentration of zinc

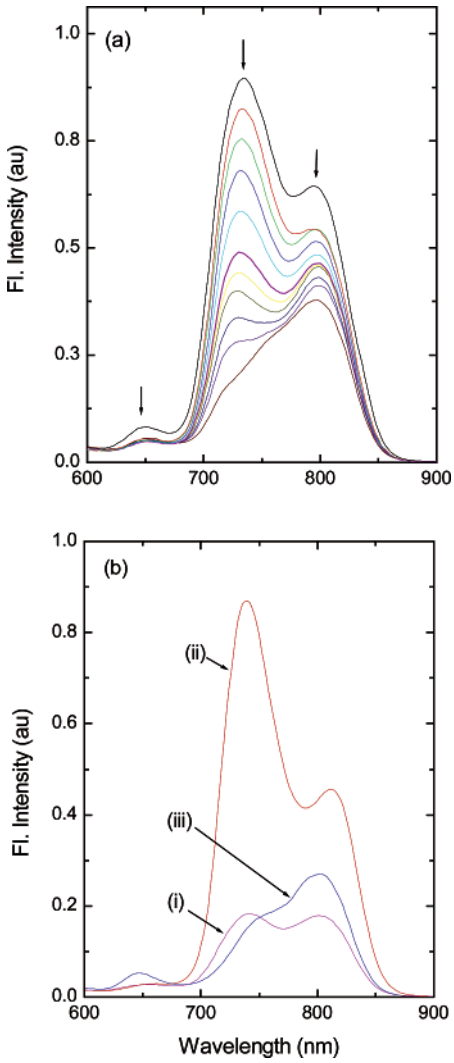

Figure 6. Fluorescence emission spectrum of (a) Py:ZnNCP (3.7 μM) on increasing addition of C_{60}Im (1.8 μM each addition) and (b) (i) ZnNCP-dimer (3.7 μM), (ii) ZnNCP-dimer (3.7 μM) on addition excess of imidazole, and (iii) ZnNCP-dimer (3.7 μM) + C_{60}Im (8.0 μM) in *o*-dichlorobenzene. The samples were excited at the Soret band position.

tetraphenylporphyrin. This observation is in agreement with a low fluorescence quantum yield reported earlier for N-confused porphyrins.[11k,22] Upon addition of C_{60}Im, the Py:ZnNCP emission was significantly quenched, as shown in Figure 6a. However, the quenching efficiency of the 734 nm band was found to be more than that of the 794 nm band.

The quenching was analyzed with Stern−Volmer plots.[25] The calculated Stern−Volmer constants, K_{SV}, values were as high as 10^3 M^{-1}. On employing the excited-state lifetime (1.6 ns) of the monomer, Py:ZnNCP, the fluorescence-quenching rate constants, k_q, were evaluated to be over 10^{12} M^{-1} s^{-1}, which was nearly 3 orders of magnitude higher than that expected for diffusion controlled-bimolecular quenching processes in the studied solvents ($\sim 5.0 \times 10^9$ M^{-1} s^{-1}),[25] suggesting that the faster intra-supramolecular processes are responsible for the fluorescence quenching.

The ZnNCP-dimer exhibited weak fluorescence emission due to self-quenching (Figure 6b); however, the emission

(24) Chitta, R.; Rogers, L. M.; Wanklyn, A.; Karr, P. A.; Kahol, P. K.; Zandler, M. E.; D'Souza, F. *Inorg. Chem.* **2004**, *43*, 6969.

(25) *Principles of Fluorescence Spectroscopy*, 2nd ed.; Lakowicz, J. R., Ed.; Kluwer Academic/Plenum: New York, 1999.

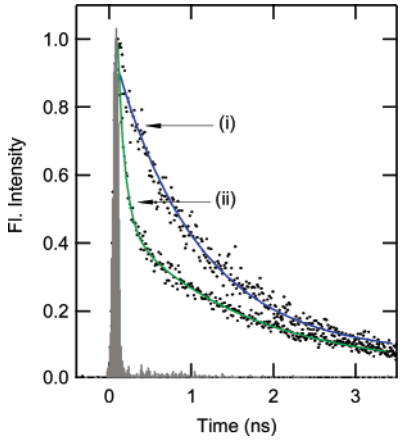

Figure 7. Fluorescence decays at 720−740 nm range of (i) ZnNCP-dimer (0.03 mM) and (ii) ZnNCP-dimer (0.03 mM) in the presence of C_{60}Im (0.10 mM) in *o*-dichlorobenzene. $\lambda_{ex} = 400$ nm.

bands were not significantly different from that of the monomer, Py:ZnNCP, due to a similar coordinating environment. Such weak fluorescence can also be attributed to the dynamic exchange of the macrocycles in the system.[22] Similar weak fluorescence was also reported for the free-base NCP.[22] In a control experiment, addition of *N*-methyl imidazole to dissociate the dimer and to form the imidazole complex, Im:ZnNCP, resulted in restoring the emission of the dimer (spectrum ii in Figure 6b). With the addition of excess of C_{60}Im to the ZnNCP-dimer, to dissociate the dimer and form the C_{60}Im:ZnNCP dyad, the emission intensity increased only slightly (spectrum iii). When compared to the emission intensity of Im:ZnNCP (axially coordinated species without electron acceptor), the quenching in Im:ZnNCP was over 70%, indicating an efficient process. These results indicate the occurrence of efficient quenching in the supramolecular dyads.

Further picosecond time-resolved emission measurements were performed to study the kinetics and mechanism of quenching in these supramolecular dyads.

Picosecond Time-Resolved Emission Studies. The time-resolved emission studies of the self-assembled conjugates tracked those of steady-state quenching measurements. Figure 7 shows the emission decay profiles of ZnNCP-dimer in the presence and absence of C_{60}Im. In the absence of C_{60}Im, ZnNCP-dimer revealed mono-exponential decay with lifetimes of 1.5 ns. The added C_{60}Im had a quenching effect on the lifetimes of the singlet excited ZnNCP. The ZnNCP emission decay in the dyad could be fitted satisfactorily by a biexponential decay curve; the lifetimes (τ_f) were 104 ps in 70% and 1980 ps in 30%. The short lifetime ($(\tau_f)_{complex}$) was predominantly due to charge-separation within the supramolecular dyad, whereas the long lifetime components are attributed to the uncomplexed ZnNCP emission.

The lifetime of the monomer, Py:ZnNCP, was found to be 1.6 ns. Upon addition of C_{60}Im to form the dyad, the ZnNCP emission revealed substantial quenching in which the decay could be fitted satisfactorily by a biexponential decay curve. The lifetimes of the two decay components were found to be 65 ps in 69% and 1960 ps in 31%, respectively, suggesting bound and free forms of the donor species in

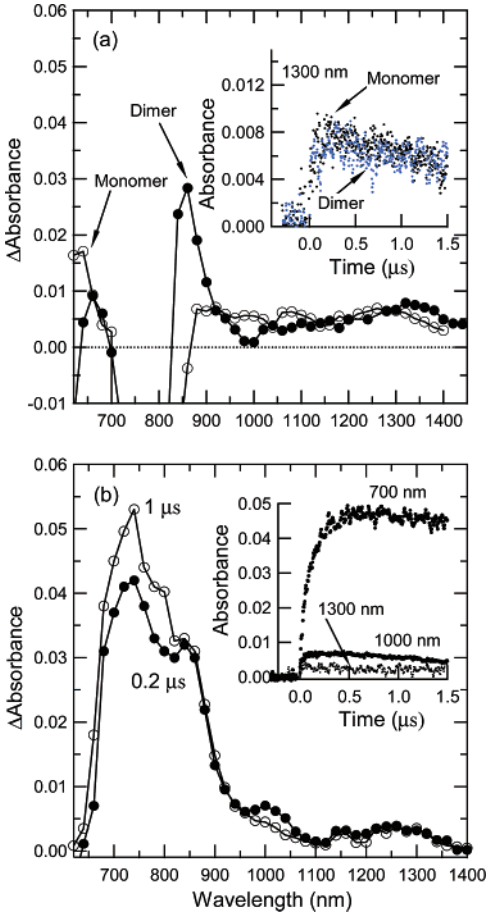

Figure 8. (a) Transient absorption spectra at 0.1 μs of Py:ZnNCP (0.03 mM) and ZnNCP-dimer (0.06 mM) in Ar-saturated *o*-dichlorobenzene obtained by 532 nm laser light excitation, respectively; (insert) time profiles for the peak at 1300 nm, (b) Transient absorption spectra of mixture of ZnNCP-dimer (0.05 mM) with C_{60}Im (0.1 mM) in Ar-saturated *o*-dichlorobenzene; (insert) time profiles at different wavelengths.

solution. The short-lifetime component is attributed to charge separation within the supramolecular dyad. The slight variations in the lifetime values of the ZnNCP-dimer and Py:ZnNCP upon complexation with C_{60}Im could be due to the presence of liberated pyridine in the latter case.

Nanosecond Transient Absorption Studies. Nanosecond transient spectra of ZnNCP-dimer and Py:ZnNCP observed after 532 nm laser excitation in deaerated *o*-DCB are shown in Figure 8a. Absorption peaks in the 600−700, 800−900, and 1100−1400 nm regions can be attributed to the triplet states of the dimer and monomer, although huge depletion was observed in the 700−800 nm region due to the emissions. Appreciable difference due to the absorption shifts of these triplet states correspond to that in steady-state absorptions. From the time profiles at 1300 nm where the depletion effect was not significant, the lifetimes of the triplet states were evaluated to be ca. 10 μs for both dimer and monomer.

On addition of C_{60}Im to the ZnNCP-dimer, new absorption spectra were observed, as shown in Figure 8b. The new transient absorption at 700 nm was attributed to the triplet state of C_{60}Im; the peak in the region from 750−900 nm was ascribed to the triplet state of ZnNCP because the depletion in the 700−800 nm region was suppressed by the

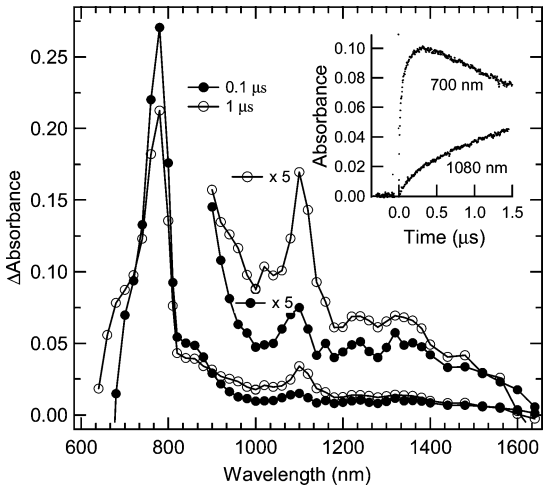

Figure 9. Transient absorption spectra of a mixture of ZnNCP-dimer (0.08 mM) with C_{60} (0.2 mM) in Ar-saturated benzonitrile obtained by 532 nm laser light excitation; (insert) time profile at 700 and 1000 nm.

shortening of the fluorescence of ZnNCP. In addition, a weak absorption appeared at 1000 nm as a shoulder, which can be attributed to the formation of $C_{60}Im^{\bullet-}$, although the absorption of $ZnNCP^{\bullet+}$ expected to appear in the 600−700 nm region was almost completely hidden by the absorptions of the triplet states of ZnNCP and $C_{60}Im$. From the time profile at 1000 nm, the lifetime was evaluated to be ca. 4 μs; however, this lifetime cannot be solely attributed to the $C_{60}Im^{\bullet-}$:$ZnNCP^{\bullet+}$ charge-separated species because of the overlaps of the slowly decaying triplet states.

To evaluate the intermolecular electron transfer, the transient absorption spectra were observed for the mixture of ZnNCP-dimer and pristine C_{60} (having no axial coordinating functionality) in polar solvent such as benzonitrile, as shown in Figure 9. Because of excess of C_{60}, the 750 nm peak was mainly attributed to the triplet state of C_{60}. With the decay of the 750 nm band, the rise of the 1080 nm band appeared, indicating the occurrence of intermolecular electron transfer via the triplet excited C_{60} to form radical ions, $C_{60}^{\bullet-}$ and $ZnNCP^{\bullet+}$-dimer. Interestingly, weak absorption in the 1200−1400 nm region was also observed which is attributable to the formation of $ZnNCP^{\bullet+}$-dimer. Therefore, the weak absorption in the 1200−1400 nm region observed for the $C_{60}Im$:ZnNCP dyad in *o*-DCB (Figure 8) can be attributed to the formation of $ZnNCP^{\bullet+}$. In conclusion, the nanosecond transient absorption spectral studies provided direct evidence for photoindueced electron transfer in the studied dyads. That is, ZnNCP cation radical bands in the 1200−1400 nm range and a fullerene anion radical band in the 1000−1100 nm range were observed.

Discussion

The results of the present investigation reveal several interesting observations. The zinc N-confused tetraphenylporphyrin monomer and dimer possess absorption bands covering most of the visible portion of the electronic spectrum with an intense band centered at 760 nm, a notable feature of N-confused porphyrins.[9−11] The self-assembled supramolecular dyads could be easily obtained by treating these porphyrin isomers with imidazole-appended fulleropyrrolidines, according to Scheme 1. A 1:1 stoichiometry of the supramolecular complex was established from the optical absorption and ESI-mass spectral studies. The binding constant values suggest fairly stable complex formation. DFT calculations at the B3LYP/3-21G(*) level revealed the electronic structure of the dyads and suggested that the charge-separated state in electron-transfer reactions of the supramolecular complex is $C_{60}Im^{\bullet-}$:$ZnNCP^{+\cdot}$. A small HOMO−LUMO gap for the dyad was predicted from these studies.

The results of the electrochemical studies were in full agreement with the B3LYP/3-21G(*) predictions. The oxidation potential of the N-confused porphyrin was found to be close to that of ferrocene and was 350 mV easier to oxidize compared to the first oxidation potential of the pyridine-coordinated zinc tetraphenylporphyrin. The driving forces for charge separation ($-\Delta G_{CS}$) was calculated according to eq 1 using the electrochemical redox and fluorescence emission data:[26]

$$-\Delta G_{CS} = E_{ox} - E_{red} - E_{0,0} - \Delta G_s \qquad (1)$$

where E_{ox} is the first oxidation potential of the N-confused porphyrin, E_{red} is the first reduction potential of the fullerene ($C_{60}Im$), $\Delta E_{0,0}$ is the energy of the 0−0 transition between the lowest excited state and the ground state of the N-confused porphyrin evaluated from the fluorescence emission peaks, and ΔG_S refers to the static energy, calculated by using the 'Dielectric Continuum Model'[24] according to eq 2.

$$\Delta G_S = e^2/(4\pi\epsilon_0\epsilon_S R_{Ct-Ct}) \qquad (2)$$

The symbols ϵ_0 and ϵ_S represent vacuum permittivity and dielectric constant of the solvent benzonitrile, respectively. Values of center-to-center distance, R_{Ct-Ct} were based on the computed structures shown in Figure 4. The calculated free-energy change for charge separation was found to be $\Delta G_{CS} = -0.96$ eV for the monomer suggesting that the charge-separation from the singlet excited ZnNCP to fullerene in the dyad is exothermic. These results predict the occurrence of rapid electron transfer in these supramolecular dyads since the ΔG_{CS} values are almost on the top region of the Marcus parabola

The charge-separation rate (k_{CS}^S) and quantum yield (Φ^S_{CS}) were evaluated from the short τ_f components according to eqs 3 and 4, a procedure commonly adopted for intramolecular electron-transfer process.[27]

$$k^S_{CS} = (1/\tau_f)_{complex} - (1/\tau_f)_{NCPZn} \qquad (3)$$

$$\Phi^S_{CS} = [(1/\tau_f)_{complex} - (1/\tau_f)_{NCPZn}]/(1/\tau_f)_{complex} \qquad (4)$$

(26) (a) Rehm, D.; Weller, A. *Isr. J. Chem.* **1970**, *7*, 259. (b) Mataga, N.; Miyasaka, H. In *Electron Transfer*; Jortner, J., Bixon, M., Eds.; John Wiley and Sons: New York, 1999; Part 2, pp 431−496.

(27) (a) D'Souza, F.; Gadde, S.; Zandler, M. E.; Arkady, K.; El-Khouly, M. E.; Fujitsuka, M.; Ito, O. *J. Phys. Chem. A* **2002**, *106*, 12393. (b) El-Khouly, M. E.; Araki, Y.; Ito, O.; Gadde, S.; McCarty, A. L.; Karr, P. A.; Zandler, M. E.; D'Souza, F. *PhysChemChemPhys* **2005**, *7*, 3163.

The calculated k_{CS}^{S} and Φ^{S}_{CS} were found to be 1.1×10^{10} s^{-1} and 0.97, respectively, when τ_f values starting from ZnNCP-dimer was employed, indicating the occurrence of efficient charge separation within the supramolecular dyad.

The charge-separated state, $C_{60}Im^{\bullet-}$:$ZnNCP^{\bullet+}$, was established by the appearance of the transient absorption bands in the 1200−1400 nm region corresponding to the $ZnNCP^{+\bullet}$ and at 1020 nm due to $C_{60}Im^{\bullet-}$. The lifetime of the charge-separated state, evaluated from the decay of the fullerene anion radical, was found to be about 4 μs, although this lifetime was considerably affected by the further long-lived triplet states. A similar value was also obtained when the 1300 nm decay corresponding to the $ZnNCP^{+\bullet}$ was monitored. The rate constant of intermolecular electron transfer from ZnNCP-dimer to the triplet state of C_{60} was evaluated to be ca. 5×10^{9} M^{-1} s^{-1} from the decay of the triplet state of C_{60} and rise of $C_{60}^{\bullet-}$. The quantum yield of electron-transfer evaluated from the ratio of the transient absorption intensities under these solution conditions was found to be about 1.

Summary

The ability of N-confused zinc tetraphenylporphyrin, a porphyrin structural isomer, to undergo photoinduced charge separation is verified by constructing supramolecular donor−acceptor dyads involving fullerene, C_{60}, as an electron acceptor. These dyads were constructed by utilizing the well-established axial coordination of imidazole-appended fullerene to the metal center of the zinc N-confused porphyrin. Both pyridine coordinated zinc N-confused porphyrin and the zinc N-confused porphyrin dimer formed 1:1 dyads whose structures were established from optical absorption and emission, ESI-mass, and electrochemical methods. The binding constant, K, was found to be 2.8×10^{4} M^{-1} for the zinc N-confused porphyrin coordinated to imidazole appended-fullerene supramolecular dyad formation. The geometric and electronic structure of the self-assembled dyad, probed using DFT B3LYP/3-21G(*) method, suggested that the charge-separated state is $C_{60}Im^{\bullet-}$:$ZnNCP^{\bullet+}$. Cyclic voltammetry studies revealed facile oxidation for the N-confused zinc porphyrins as compared to the parent zinc tetraphenylporphyrin, and calculated free-energy change revealed that the electron-transfer reaction to be highly exothermic. Steady-state and time-resolved emission studies revealed efficient quenching of the singlet excited dyad, $C_{60}Im$:$^{1}ZnNCP^{*}$. The calculated k_{CS}^{S} and Φ^{S}_{C} were found to be 1.1×10^{10} s^{-1} and 0.97, respectively, indicating the occurrence of efficient charge separation within the supramolecular dyad, which was further experimentally proved by the nanosecond transient absorption spectra measurements.

Acknowledgment. This work is supported by the National Science Foundation (Grant No. 0453464 to F.D.), the donors of the Petroleum Research Fund administered by the American Chemical Society, and Grants-in-Aid for Scientific Research on Primary Area (417) from the Ministry of Education, Science, Sport and Culture of Japan.

Supporting Information Available: Synthetic details of ZnNCP and ZnNCP-dimer. This material is available free of charge via the Internet at http://pubs.acs.org.

IC0601687